

Finite-time control for uncertain systems and application to flight control*

Fang Wang^{a,1}, Jianmei Wang^a, Kun Wang^a, Changchun Hua^b,
Qun Zong^c

^aSchool of Science, Yanshan University,
Qinhuangdao, China
wangfang@ysu.edu.cn

^bSchool of Electrical and Engineering,
Yanshan University,
Qinhuangdao, China

^cSchool of Electrical and Information Engineering,
Tianjin University,
Tianjin, China

Received: September 3, 2018 / **Revised:** June 7, 2019 / **Published online:** March 2, 2020

Abstract. In this paper, the finite-time control design problem for a class of nonlinear systems with matched and mismatched uncertainty is addressed. The finite-time control scheme is designed by integrating multi power reaching (MPR) law and finite-time disturbance observer (FTDO) into integral sliding mode control, where a novel sliding surface is designed, and the FTDO is applied to estimate the uncertainty. Then the fixed-time reachability of the MPR law is analyzed, and the finite-time stability of the closed-loop system is proven in the framework of Lyapunov stability theory. Finally, numerical simulation and the application to the flight control of hypersonic vehicle (HSV) are provided to show the effectiveness of the designed controller.

Keywords: finite-time control, MPR law, matched and mismatched uncertainty, HSV.

1 Introduction

It is necessary to take uncertainties into account when considering the system performance, since system performance degradation and instability are caused by uncertainties. Sliding mode control (SMC) [29] is probably the most popular approaches for dealing with bounded uncertainties, and it can achieve the finite-time stabilization of the sliding variable through switching control [19]. Besides, it has been regarded as one of the effective robust control approaches owing to its many various advantages, which include

*This research was supported by Natural Science Foundation of Hebei Province of China under grant No. F2017203130, National Natural Science Foundation of China under grant No. 61673294.

¹Corresponding author.

its invariance to system uncertainties and external disturbances, i.e., the strong robustness [7, 28]. And thereby, the research on SMC design of uncertain systems and application to engineering systems [23–26] has attracted a lot of attention. The convergence of the traditional linear sliding mode control (LSMC) is asymptotically stable. Compared with LSMC, terminal sliding mode control (TSMC) converges fleetly in finite time [14], so it had been widely proposed in the literature. However, the conventional TSMC has singularity problem. To avoid this problem, the nonsingular TSMC (NTSMC) was proposed in [8], but it is only suitable for the second-order and some special high-order systems. A continuous NTSMC scheme [35] was designed for a system with the mismatched uncertainty in which the mismatched uncertainty was handled by a FTDO, and the system achieved stable in finite time. However, the sliding surface needs to be designed for second-order and n th-order ($n > 2$) system, respectively. Then in [10], a continuous NTSMC strategy was proposed, but it did not provide convergence analysis. Furthermore, a controller, which combined super-twisting algorithm and TSMC, was proposed in [12]. Based on the finite-time convergence and robustness properties, the stability analysis was only suitable for the first- or second-order system. A single exponential reaching law-based SMC scheme [39] made the system stable in finite time, while the chattering problem cannot be eliminated completely.

System uncertainty includes matched uncertainty that acts on the system via the input channel, and mismatched uncertainty that contains perturbations in the system parameters. SMC is robust for matched uncertainty, but it is still a challenge to design SMC scheme for systems with the mismatched uncertainty, since the uncertain system dynamics are influenced even after reaching the sliding surface [17, 37]. For the importance of tackling mismatched uncertainties in practical applications, many control approaches have been proposed to address the problem of mismatched uncertainties [32, 33, 38]. The combination of SMC with other methods that provide estimate of uncertainties enables a reduction in the magnitude of the discontinuous component in control and thereby offers the possibility of mitigating the chattering in control input [11]. Disturbance observer (DO) technique is one such strategy that has been integrated with SMC for nonlinear systems with mismatched uncertainty [36]. The DO technique has been proved to be effective in compensating the effects of unknown external disturbances and model uncertainties in control systems [6]. Besides, DO-based control method can provide a feasible way in improving robustness and handling the unknown disturbances or uncertainties of nonlinear systems. As we know, although SMC behaves the characteristic of robustness, the chattering problem is its main disadvantage. A lot of approaches are applied to eliminate the chattering problem, such as high-order SMC, the replacement of sign function with sigmoid function or saturated function, reaching law-based control [15, 40]. The reaching law-based control achieves the improvement of the dynamic performance for the reaching phase and alleviates the chattering problem to some extent.

In this paper, the control design problem of a class of nonlinear systems with matched and mismatched uncertainty is addressed by combining FTDO, MPR law and SMC. The contribution can be concluded as follows.

The fixed-time reachability of the MPR law is firstly analyzed, and the upper bound of the reachability time is obtained. Moreover, the MPR law is combined with FTDO

technique to ensure the system state converges to zero in finite time even the system is affected by the uncertainty.

In addition, the matched and mismatched uncertainty is tackled by the FTDO. Then the sliding mode controller is designed based on the FTDO, the MPR law and the integral sliding surface. It avoids the chattering problem caused by the sign function existed in traditional SMC.

To proceed, the output tracking error is proven to converge to zero in finite time. At the level of simulation, the fastest stability of the designed control strategy is testified by comparing it with other two methods. Its effectiveness is further evaluated by the application to altitude and velocity tracking control of HSV.

The outline of this paper is as follows. Section 2 introduces the problem formulation and preliminaries, which are subsequently being used in controller design and stability analysis. The FTDO-based SMC scheme and the stability analysis of the closed-loop system are given in Section 3. Then in Section 4, the effectiveness of the proposed scheme is evaluated by numerical simulations. Finally, conclusions are shown in Section 5.

2 System description and preliminaries

2.1 System description

Consider a class of nonlinear systems given by

$$\begin{aligned} \dot{x}_i &= x_{i+1} + d_i(x, t), \quad i = 1, 2, \dots, n-1, \\ \dot{x}_n &= f(x) + g(x)u + d_n(x, t), \\ y &= x_1, \end{aligned} \quad (1)$$

where x_1, x_2, \dots, x_n represent the system states, $x = [x_1, x_2, \dots, x_n]^T$, u and y are the control input and the output, respectively. $f(x)$, $g(x)$ are smooth functions and $g(x) \neq 0$, $d_i(x, t)$, $i = 1, 2, \dots, n-1$, and $d_n(x, t)$ represent the mismatched and matched disturbance, respectively. They may include external unmeasurable and/or state dependent disturbances, uncertainties and nonlinearities.

Assumption 1. The output reference command and its time derivative are continuous and bounded, i.e., x_{1d} , \dot{x}_{1d} are continuous and bounded.

Assumption 2. For the system disturbances $d_i(x, t)$, $i = 1, 2, \dots, n$, there exist unknown positive constants μ_i so that $|d_i(x, t)| \leq \mu_i$, and $d_i(\bar{x}_i, t)$ is $(n-i+1)$ th differentiable.

The control objective is to propose the sliding mode control law which combining the MPR law and FTDO such that the closed loop system achieves the stable tracking in finite time.

2.2 Preliminaries

The lemmas and definitions, which will be used in Section 3, are given here.

Lemma 1. (See [1].) Consider the following system:

$$\dot{x} = f(x), \quad x \in \mathbb{R}, \quad f(0) = 0.$$

Suppose that there is a continuous function $V(x) : U \rightarrow \mathbb{R}$ such that

- (i) $V(x)$ is positive definite.
- (ii) There are real numbers $c > 0$, $\alpha \in (0, 1)$ and an open neighborhood $U_0 \in U$ of the origin such that $\dot{V}(x) + cV^\alpha(x) \leq 0$, $x \in U_0 \setminus \{0\}$.

Then the origin is a finite-time stable equilibrium of system. If $U = U_0 = \mathbb{R}^n$, the origin is a globally finite-time stable equilibrium of system.

Lemma 2. (See [2].) Consider the following system:

$$\begin{aligned} \dot{x}_i &= x_{i+1}, \quad i = 1, 2, \dots, n - 1, \\ \dot{x}_n &= u. \end{aligned}$$

If the controller is designed as

$$\begin{aligned} u &= -k_1 \operatorname{sgn} x_1 |x_1|^{\alpha_1} - k_2 \operatorname{sgn} x_2 |x_2|^{\alpha_2} - k_3 \operatorname{sgn} x_3 |x_3|^{\alpha_3} \\ &\quad - \dots - k_n \operatorname{sgn} x_n |x_n|^{\alpha_n}, \end{aligned}$$

under the control input, the closed-loop system is globally finite-time stable, where $\alpha_{i-1} = \alpha_i \alpha_{i+1} / (2\alpha_{i+1} - \alpha_i)$, $i = 2, 3, \dots, n$, $\alpha_n = \alpha$, $\alpha \in (1 - \varepsilon, 1)$, $\varepsilon \in (0, 1)$, $\alpha_{n+1} = 1$, and k_1, k_2, \dots, k_n ensure that $s^n + k_n s^{n-1} + \dots + k_1 = 0$ is Hurwitz.

Definition 1. (See [18].) Consider the following system:

$$\dot{x} = f(x, t), \quad x \in \mathbb{R}^n, \quad x(0) = x_0, \tag{2}$$

where $f(x, t) \in \mathbb{R}^n \times \mathbb{R}_+ \rightarrow \mathbb{R}^n$ is a nonlinear function, which can be discontinuous. Assume the origin is an equilibrium point of (2). The origin of (2) is said to be fixed-time stable if it is globally finite-time stable and the settling time function $T(x_0)$ is bounded, i.e., there is $T_{\max} > 0$ such that $T(x_0) \leq T_{\max}$ for all $x_0 \in \mathbb{R}^n$.

3 MPR law-based SMC design

In this section, the SMC scheme is designed for uncertain system based on FTDO and the MPR law, where the FTDO is used to handling uncertainties, and the MPR law is employed to alleviate the chattering problem of SMC.

3.1 Fixed-time reachability of the MPR law

We adopt the following MPR law [40]:

$$\dot{s} = -c_1 |s|^{\beta_1} \operatorname{sgn} s - c_2 |s|^{\beta_2} \operatorname{sgn} s - c_3 |s|^{\beta_3} \operatorname{sgn} s - c_4 s, \tag{3}$$

where $c_i > 0, i = 1, \dots, 4, \beta_1 > 1, 0 < \beta_2 < 1,$

$$\beta_3 = \begin{cases} \max\{\beta_1, |s|\}, & |s| \geq 1, \\ \min\{\beta_2, |s|\} & \text{else.} \end{cases}$$

There are three exponential terms in (3), which are used to adjust the convergence process to make the system has a faster convergence speed obviously. The finite-time reachability of the above reaching law is analyzed in [40]. In what follows, the further analysis is done to show that it behaves fixed-time reachability.

As demonstrated in [40], for the continuous system without uncertainty, under the MPR law (3), the sliding variable reaches the sliding surface $s = 0$ in finite time T_0 , which satisfies

$$T_0 \leq T_1 + T_2 + T_3 + T_4$$

with

$$\begin{aligned} T_1 &= \frac{1}{(1 - \beta_1)c_4} \left[\ln \left(\beta_1^{1-\beta_1} + \frac{c_1}{c_4} \operatorname{sgn} s_0 \right) - \ln \left(s_0^{1-\beta_1} + \frac{c_1}{c_4} \operatorname{sgn} s_0 \right) \right], \\ T_2 &= \frac{1}{(1 - \beta_1)c_4} \left[\ln \left(1 + \frac{c_1 + c_3}{c_4} \operatorname{sgn} s_0 \right) - \ln \left(\beta_1^{1-\beta_1} + \frac{c_1 + c_3}{c_4} \operatorname{sgn} s_0 \right) \right], \\ T_3 &= \frac{1}{(\beta_2 - 1)c_4} \left[\ln \left(\beta_2^{1-\beta_2} + \frac{c_2}{c_4} \operatorname{sgn} s_0 \right) - \ln \left(1 + \frac{c_2}{c_4} \operatorname{sgn} s_0 \right) \right], \\ T_4 &= \frac{1}{(\beta_2 - 1)c_4} \left[\ln \left(1 + \frac{c_2 + c_3}{c_4} \operatorname{sgn} s_0 \right) - \ln \left(\beta_2^{1-\beta_2} + \frac{c_2 + c_3}{c_4} \operatorname{sgn} s_0 \right) \right], \end{aligned} \tag{4}$$

where s_0 is the initial value of s .

To proceed, we will prove that the reaching phase of (3) is completed in fixed time, i.e., the sliding variable s reaches the sliding surface $s = 0$ in fixed time.

Theorem 1. *Under the MPR law (3), the reachability of the sliding variable s can be ensured in a fixed time T , which satisfies $T \leq T'_{\max} = \max\{T'_{1\max}, T'_{2\max}\}$, where*

$$\begin{aligned} T'_{1\max} &= \frac{1}{(\beta_1 - 1)c_4} \ln \frac{c_4\beta_1^{1-\beta_1} + c_1 + c_3}{c_4\beta_1^{1-\beta_1} + c_1} + \frac{1}{(1 - \beta_2)c_4} \ln \frac{\beta_2^{1-\beta_2}c_4 + c_2 + c_3}{c_4}, \\ T'_{2\max} &= \frac{1}{(\beta_1 - 1)c_4} \ln \frac{c_4(-1)^{1-\beta_1} - c_1}{c_4\beta_1^{1-\beta_1} - c_1} \frac{c_4\beta_1^{1-\beta_1} - (c_1 + c_3)}{c_4 - (c_1 + c_3)} \\ &\quad + \frac{1}{(1 - \beta_2)c_4} \ln \left[\frac{c_4 - c_2}{\beta_2^{1-\beta_2}c_4 - c_2} \frac{\beta_2^{1-\beta_2}c_4 - (c_2 + c_3)}{c_4 - (c_2 + c_3)} \right]. \end{aligned}$$

Proof. We carry out the analysis into two cases, one is $s_0 > 0$, another is $s_0 < 0$.

Case 1: $s_0 > 0$. Without loss of generality, assume that $s_0 > \beta_1$, the reaching phase of s can be completed through four phases as follows:

$$s_0 \longrightarrow \beta_1 \longrightarrow 1 \longrightarrow \beta_2 \longrightarrow 0.$$

(a) For the first two phases, $s_0 \rightarrow \beta_1 \rightarrow 1$, from (4), the reaching time T_{11} is

$$T_{11} = T_1 + T_2 = \frac{1}{(\beta_1 - 1)c_4} \ln \frac{s_0^{1-\beta_1} + \frac{c_1}{c_4}}{\beta_1^{1-\beta_1} + \frac{c_1}{c_4}} + \frac{1}{(\beta_1 - 1)c_4} \ln \frac{\beta_1^{1-\beta_1} + \frac{c_1+c_3}{c_4}}{1 + \frac{c_1+c_3}{c_4}}.$$

The derivative of T_{11} with respect to s_0 is

$$\frac{dT_{11}}{ds_0} = -\frac{s_0^{-\beta_1}}{c_4} \frac{\beta_1^{1-\beta_1} + \frac{c_1}{c_4}}{s_0^{1-\beta_1} + \frac{c_1}{c_4}},$$

since $s_0 > 0, \beta_1 > 1, dT_{11}/ds_0 < 0$, which induces that T_{11} is monotone decreasing when s_0 decreases to 1. Thus, T_{11} is governed by the following inequality:

$$T_{11} \leq T_{11}|_{s_0=1} = \frac{1}{(\beta_1 - 1)c_4} \ln \frac{c_4 + c_1}{c_4\beta_1^{1-\beta_1} + c_1} \frac{c_4\beta_1^{1-\beta_1} + c_1 + c_3}{c_4 + c_1 + c_3} \leq \frac{1}{(\beta_1 - 1)c_4} \ln \frac{c_4\beta_1^{1-\beta_1} + c_1 + c_3}{c_4\beta_1^{1-\beta_1} + c_1}.$$

(b) For the last two phases, $1 \rightarrow \beta_2 \rightarrow 0$, from (4), the reaching time T_{12} is

$$T_{12} = T_3 + T_4 = \frac{1}{(\beta_2 - 1)c_4} \ln \frac{\beta_2^{1-\beta_2} + \frac{c_2}{c_4}}{1 + \frac{c_2}{c_4}} + \frac{1}{(\beta_2 - 1)c_4} \ln \frac{1 + \frac{c_2+c_3}{c_4}}{\beta_2^{1-\beta_2} + \frac{c_2+c_3}{c_4}} = \frac{1}{(1 - \beta_2)c_4} \ln \frac{c_4 + c_2}{\beta_2^{1-\beta_2}c_4 + c_2} \frac{\beta_2^{1-\beta_2}c_4 + c_2 + c_3}{c_4 + c_2 + c_3} \leq \frac{1}{(1 - \beta_2)c_4} \ln \frac{\beta_2^{1-\beta_2}c_4 + c_2 + c_3}{c_4 + c_2 + c_3} \leq \frac{1}{(1 - \beta_2)c_4} \ln \frac{\beta_2^{1-\beta_2}c_4 + c_2 + c_3}{c_4}.$$

Based on above analysis, when $s_0 > 0$, the sliding variable s will reach the sliding surface $s = 0$ in the fixed time T'_1 , which yields

$$T'_1 = T_{11} + T_{12} \leq T'_{1 \max} = \frac{1}{(\beta_1 - 1)c_4} \ln \frac{c_4\beta_1^{1-\beta_1} + c_1 + c_3}{c_4\beta_1^{1-\beta_1} + c_1} + \frac{1}{(1 - \beta_2)c_4} \ln \frac{\beta_2^{1-\beta_2}c_4 + c_2 + c_3}{c_4}. \tag{5}$$

Case 2: $s_0 < 0$. We assume that $s_0 < -\beta_1$, and the reaching phase of sliding variable s can be divided into following four phases:

$$s_0 \rightarrow -\beta_1 \rightarrow -1 \rightarrow -\beta_2 \rightarrow 0.$$

(a) For the first two phases, $s_0 \rightarrow -\beta_1 \rightarrow -1$, the reaching time T_{21} is

$$T_{21} = T_1 + T_2 = \frac{1}{(\beta_1 - 1)c_4} \ln \frac{s_0^{1-\beta_1} - \frac{c_1}{c_4}}{\beta_1^{1-\beta_1} - \frac{c_1}{c_4}} + \frac{1}{(\beta_1 - 1)c_4} \ln \frac{\beta_1^{1-\beta_1} - \frac{c_1+c_3}{c_4}}{1 - \frac{c_1+c_3}{c_4}}, \tag{6}$$

and the derivative of T_{21} with respect to s_0 is

$$\frac{dT_{21}}{ds_0} = -\frac{s_0^{-\beta_1}}{c_4} \frac{\beta_1^{1-\beta_1} - \frac{c_1}{c_4}}{s_0^{1-\beta_1} - \frac{c_1}{c_4}}.$$

From equations (4) and (6) we have $\beta_1^{1-\beta_1} > c_1/c_4$, $s_0^{1-\beta_1} > c_1/c_4$, $\beta_1^{1-\beta_1} > s_0^{1-\beta_1}$, then $s_0^{1-\beta_1} > c_1/c_4 > 0$, and $s_0^{-\beta_1} = s_0^{1-\beta_1}/s_0 < 0$, $\beta_1 > 1$, thereby, $dT_{21}/ds_0 > 0$. Then we obtain that T_{21} is monotone increasing when $s_0 \in (-\infty, -1]$, and it satisfies

$$\begin{aligned} T_{21} &\leq T_{21}|_{s_0=-1} \\ &= \frac{1}{(\beta_1 - 1)c_4} \ln \frac{c_4(-1)^{1-\beta_1} - c_1}{c_4\beta_1^{1-\beta_1} - c_1} \frac{c_4\beta_1^{1-\beta_1} - (c_1 + c_3)}{c_4 - (c_1 + c_3)}. \end{aligned}$$

(b) For the last two phases, the reaching process of sliding variable s is $-1 \rightarrow -\beta_2 \rightarrow 0$, the reaching time T_{22} is

$$\begin{aligned} T_{22} = T_3 + T_4 &= \frac{1}{(\beta_2 - 1)c_4} \ln \frac{\beta_2^{1-\beta_2} - \frac{c_2}{c_4}}{1 - \frac{c_2}{c_4}} + \frac{1}{(\beta_2 - 1)c_4} \ln \frac{1 - \frac{c_2+c_3}{c_4}}{\beta_2^{1-\beta_2} - \frac{c_2+c_3}{c_4}} \\ &= \frac{1}{(1 - \beta_2)c_4} \ln \frac{1 - \frac{c_2}{c_4}}{\beta_2^{1-\beta_2} - \frac{c_2}{c_4}} \frac{\beta_2^{1-\beta_2} - \frac{c_2+c_3}{c_4}}{1 - \frac{c_2+c_3}{c_4}} \\ &\leq \frac{1}{(1 - \beta_2)c_4} \ln \frac{c_4 - c_2}{\beta_2^{1-\beta_2}c_4 - c_2} \frac{\beta_2^{1-\beta_2}c_4 - (c_2 + c_3)}{c_4 - (c_2 + c_3)}. \end{aligned}$$

As shown in above equation, when $s_0 < 0$, s will reach the sliding surface $s = 0$ in a fixed time T'_2 , which is

$$\begin{aligned} T'_2 &= T_{21} + T_{22} \\ &\leq T'_{2\max} = \frac{1}{(\beta_1 - 1)c_4} \ln \frac{c_4(-1)^{1-\beta_1} - c_1}{c_4\beta_1^{1-\beta_1} - c_1} \frac{c_4\beta_1^{1-\beta_1} - (c_1 + c_3)}{c_4 - (c_1 + c_3)} \\ &\quad + \frac{1}{(1 - \beta_2)c_4} \ln \frac{c_4 - c_2}{\beta_2^{1-\beta_2}c_4 - c_2} \frac{\beta_2^{1-\beta_2}c_4 - (c_2 + c_3)}{c_4 - (c_2 + c_3)}. \end{aligned} \tag{7}$$

From above analysis, the sliding variable s reaches the sliding surface $s = 0$ in a fixed time T , which satisfies $T \leq T'_{\max} = \max\{T'_{1\max}, T'_{2\max}\}$. As shown in (5) and (7), T'_{\max} has no relationship with s_0 , so referred to [32], the sliding variable s can reach the sliding surface $s = 0$ in the fixed time. The proof is completed. \square

Remark 1. Although in this paper, we adopt the MPR law proposed in [40], the difference of this paper is as follows. In [40], authors had analyzed that the MPR law (3) can assure the stability of the system without uncertainty in finite time, while in this paper, we further analyze and obtain the fixed-time stability. Furthermore, in [40], when the system is affected by uncertainty or disturbance, the MPR law (3) makes the system state converges to a neighborhood around equilibrium point in finite time, while in this paper, we combine the MPR law with FTDO technique to guarantee that the system state converges to zero in finite time. The detail procedure will be shown in the following section.

3.2 Control law design

In this section, we will incorporate the MPR law (3) and FTDO into SMC to design controller for the uncertain system (1).

The tracking error of system (1) is defined as

$$e = x_1 - x_{1d}, \tag{8}$$

where x_{1d} is the reference command of x_1 .

From (8) and inspired by [35], a novel sliding surface is designed as

$$s = e^{[n-1]} + \int_0^\sigma \sum_{i=0}^{n-1} l_i \operatorname{sgn} e^{[i]} |e^{[i]}|^{\omega_i} d\sigma, \tag{9}$$

where $\omega_{i-1} = \omega_i \omega_{i+1} / (2\omega_{i+1} - \omega_i)$ ($i = 2, \dots, n$), $\omega_{n+1} = 1$, $\omega_n = \omega_0 \in (1 - \varepsilon, 1)$, $\varepsilon \in (0, 1)$, $l_i > 0$ ($i = 0, 1, \dots, n - 1$), and the polynomial $\lambda^{n-1} + l_{n-1}\lambda^{n-2} + \dots + l_1\lambda + l_0$ is Hurwitz.

Remark 2. The difference of this paper from [35] is as follows. (a) The controller of this paper is designed by integrating MPR law and FTDO into SMC, which guarantees the finite-time stability of the system, and the tracking error converges to zero in finite time. (b) Based on the applied MPR law, the fixed-time reachability of the sliding variable is analyzed, and the finite-time stability of the system is achieved. The time derivative of (9) along (1) is

$$\dot{s} = f(x) + g(x)u + \sum_{i=1}^n d_i^{[n-i]} - x_{1d}^{[n]} + \sum_{i=0}^{n-1} l_i \operatorname{sgn} e^{[i]} |e^{[i]}|^{\omega_i} \tag{10}$$

In (10), the terms $d_i^{[n-i]}$ represent the $(n - i)$ th time derivative of the i th disturbance, and $\hat{d}_i^{[n-i]}$ are their estimate, which are provide by the FTDO proposed in [5, 16, 20], and its formulation is

$$\begin{aligned} \hat{x}_i &= z_0^i, \quad \hat{d}_i = z_1^i, \quad \hat{\dot{d}}_i = z_2^i, \quad \dots, \quad d_i^{[n-i]} = z_{n-i+1}^i, \\ \dot{z}_0^i &= v_0^i + f_i(x, u), \\ v_0^i &= -\eta_0^i L_i^{1/(n-i+2)} |z_0^i - x_i|^{(n-i+1)/(n-i+2)} + \operatorname{sgn}(z_0^i - x_i) + z_1^i, \\ \dot{z}_1^i &= v_1^i, \\ v_1^i &= -\eta_1^i L_i^{1/(n-i+1)} |z_1^i - v_0^i|^{(n-i)/(n-i+1)} \operatorname{sgn}(z_1^i - v_0^i) + z_2^i, \\ &\dots \\ v_j^i &= -\eta_j^i L_i^{1/(n-i+2-j)} |z_j^i - v_{j-1}^i|^{(n-i+1-j)/(n-i+2-j)} \operatorname{sgn}(z_j^i - v_{j-1}^i) + z_{j+1}^i, \\ &\dots \\ \dot{z}_{n-i+1}^i &= v_{n-i+1}^i, \\ v_{n-i+1}^i &= -\eta_{n-i+1}^i L_i \operatorname{sgn}(z_{n-i+1}^i - v_{n-i}^i) \end{aligned} \tag{11}$$

with $i = 1, 2, \dots, n$ and $j = 0, 1, 2, \dots, n - i + 1$, $f_i(x, u) = x_{i+1}$, $i = 1, \dots, n - 1$, $f_n(x, u) = f(x) + g(x)u$, and $\eta_j^i > 0$ is the observer coefficients to be designed, whose design procedure can be referred to [16]. And the larger the parameters, the faster the convergence and the higher sensitivity to input noises and the sampling step [16], and the trade-off should be made when designing these coefficients.

Define the estimate errors $e_0^i = z_0^i - x_i$, $e_j^i = z_j^i - d_i^{[j-1]}$, then the dynamic of the estimate errors are governed by

$$\begin{aligned} \dot{e}_0^i &= -\eta_0^i L_i^{1/(n-i+2)} |e_0^i|^{(n-i+1)/(n-i+2)} \operatorname{sgn}(e_0^i) + e_1^i, \\ &\dots \\ \dot{e}_j^i &= -\eta_j^i L_i^{1/(n-i+2-j)} |e_j^i - \dot{e}_{j-1}^i|^{(n-i+1-j)/(n-i+2-j)} \\ &\quad \times \operatorname{sgn}(e_j^i - \dot{e}_{j-1}^i) + e_{j+1}^i, \\ \dot{e}_{n-i+1}^i &\in -\eta_{n-i+1}^i L_i \operatorname{sgn}(e_{n-i+1}^i - \dot{e}_{n-i}^i) + [-L_i, L_i]. \end{aligned} \tag{12}$$

Assume that the disturbance satisfies Assumption 2, then it follows from [5, 16, 20] that the observer error system (12) is finite-time stable, i.e., there is a time constant $T_e = T_0$ satisfies that $e_j^i = 0$ for $t > T_e$.

Combining with the MPR law(3), the control input is designed as

$$\begin{aligned} u &= -g^{-1}(x) \left[f(x) + \sum_{i=1}^n \hat{d}_i^{[n-i]} - x_{1d}^{[n]} + \sum_{i=0}^{n-1} l_i \operatorname{sgn} e^{[i]} |e^{[i]}|^{\omega_i} \right. \\ &\quad \left. + c_1 |s|^{\beta_1} \operatorname{sgn} s + c_2 |s|^{\beta_2} \operatorname{sgn} s + c_3 |s|^{\beta_3} \operatorname{sgn} s + c_4 s \right]. \end{aligned} \tag{13}$$

So substituting (13) into (10), (3) holds, and as the analysis mentioned in Section 3.1, s reaches the sliding surface $s = 0$ in fixed time.

Remark 3. It is known that the sign function in traditional SMC induces the chattering problem. Though (13) includes sign function, the term $|s_{\theta i}|^{k_{\theta i}} \operatorname{sign}(s_{\theta i})$ ($i = 1, 2, 3$) is a continuous function [2], which alleviates the chattering problem, and it also can be clearly seen from the simulation results in Section 4.

Remark 4. There are many other robust control schemes to deal with uncertainty. The main differences of DO-based control approach from other robust approaches can be concluded as follows. At first, since the DO-based compensation is added to improve the robustness and disturbance attenuation after the base line controller is developed, there is no change to the base line controller. Secondly, DO-based control method is not a worst case-based design while most of the existed robust control approaches are worst case-based design, which has been criticized as being “over-conservative”, and promising robustness is achieved with the price of degraded nominal performance. Besides, for DO-based control approach, the nominal performance of the base line controller is recovered in the absence of disturbances or uncertainties.

3.3 Stability analysis

In this subsection, the stability analysis of the closed-loop system will be shown in the framework of Lyapunov theory, and it is concluded as the following theorem.

Theorem 2. Consider the nonlinear system (1), under Assumptions 1, 2, with FTDO (11), the sliding surface (9), and the designed sliding mode controller (13), the tracking error e converges to zero in finite time.

Proof. Choose the Lyapunov function as

$$V = \frac{1}{2} \sum_{i=0}^{n-1} (e^{[i]})^2. \quad (14)$$

The time derivative of (14) yields

$$\dot{V} = \sum_{i=0}^{n-1} e^{[i]} e^{[i+1]} \leq \frac{e^2}{2} + \sum_{i=1}^{n-1} \frac{3(e^{[i]})^2}{2} + \frac{(e^{[n]})^2}{2}. \quad (15)$$

For the last term $e^{[n]} = [\dot{s} - \sum_{i=0}^{n-1} l_i \operatorname{sgn} e^{[i]} |e^{[i]}|^{\omega_i}]$, from (10) and (13), $e^{[n]} = -c_1 |s|^{\beta_1+1} - c_2 |s|^{\beta_2+1} - c_3 |s|^{\beta_3+1} - c_4 s^2 + \sum_{i=1}^n e_{n-i}^i - \sum_{i=0}^{n-1} l_i \operatorname{sgn} e^{[i]} |e^{[i]}|^{\omega_i}$, so (15) satisfies

$$\begin{aligned} \dot{V} \leq & \frac{e^2}{2} + \sum_{i=1}^{n-1} \frac{3(e^{[i]})^2}{2} + \frac{5}{2} (c_1^2 |s|^{2\beta_1} + c_2^2 |s|^{2\beta_2} + c_3^2 |s|^{2\beta_3} + c_4^2 |s|^2) s^2 \\ & + 2 \left(\sum_{i=1}^n e_{n-i}^i \right)^2 + 2 \left(\sum_{i=0}^{n-1} l_i \operatorname{sgn} e^{[i]} |e^{[i]}|^{\omega_i} \right)^2. \end{aligned}$$

Since $|e^{[i]}|^{\omega_i} < (1 + |e^{[i]}|)$ and by invoking the Cauchy–Schwarz inequality [27] $(a_1 + \dots + a_n)^2 \leq n(a_1^2 + \dots + a_n^2)$, above inequality yields

$$\begin{aligned} \dot{V} \leq & \frac{5}{2} (c_1^2 |s|^{2\beta_1} + c_2^2 |s|^{2\beta_2} + c_3^2 |s|^{2\beta_3} + c_4^2 |s|^2) s^2 + \frac{3}{2} \sum_{i=0}^{n-1} (e^{[i]})^2 \\ & + \frac{4}{n-1} \sum_{i=0}^{n-1} l_i^2 (e^{[i]})^2 + 2 \sum_{i=1}^n e_{n-i}^i + 4 \left(\sum_{i=0}^{n-1} l_i \right)^2. \end{aligned} \quad (16)$$

(a) If $|s| > 1$, $|s| < |s_0|$, then (16) satisfies

$$\begin{aligned} \dot{V} \leq & \frac{5}{2} (c_1^2 |s_0|^{2\beta_1} + c_2^2 |s_0|^{2\beta_2} + c_3^2 |s_0|^{2\beta_3} + c_4^2 |s_0|^2) s^2 \\ & + \sum_{i=0}^{n-1} \left(\frac{3}{2} + \frac{4}{n-1} l_i^2 \right) (e^{[i]})^2 + \frac{1}{2} \sum_{i=1}^n e_{n-i}^i + 4 \left(\sum_{i=0}^{n-1} l_i \right)^2. \end{aligned} \quad (17)$$

(b) If $|s| \leq 1$, then (16) can be rewritten as

$$\begin{aligned} \dot{V} &\leq \frac{5}{2}(c_1^2 + c_2^2 + c_3^2 + c_4^2)s^2 \\ &\quad + \sum_{i=0}^{n-1} \left(\frac{3}{2} + \frac{4}{n-1}l_i^2 \right) (e^{[i]})^2 + \frac{1}{2} \sum_{i=1}^n e_{n-i}^i + 4 \left(\sum_{i=0}^{n-1} l_i \right)^2. \end{aligned} \tag{18}$$

Based on (17) and (18), (16) can be expressed as

$$\begin{aligned} \dot{V} &\leq K_1 s^2 + \left(\frac{3}{2} + \frac{4}{n-1}l_i^2 \right) \sum_{i=0}^{n-1} (e^{[i]})^2 + \frac{5}{2} \sum_{i=1}^n e_{n-i}^i + 4 \left(\sum_{i=0}^{n-1} l_i \right)^2 \\ &\leq KV + C, \end{aligned} \tag{19}$$

where $K = \max\{3 + 8l_i^2/(n-1), K_1\}$, $i = 1, \dots, n$, $K_1 = \max\{K_2, K_3\}$, $C = \sum_{i=1}^n e_{n-i}^i/2 + 4(\sum_{i=0}^{n-1} l_i)^2$, $K_2 = 5(c_1^2 + c_2^2 + c_3^2 + c_4^2)$, $K_3 = 5(c_1^2|s_0|^{2\beta_1} + c_2^2|s_0|^{2\beta_2} + c_3^2|s_0|^{2\beta_3} + c_4^2|s_0|^2)$.

As shown in (12), the estimate error e_{n-i}^i will converge to zero in finite time. It implies that in (19), C is bounded, then referred to [27], V and $e^{[i]}$, $i = 1, 2, \dots, n$, will not escape to infinity time before the convergence of observer error dynamics.

According to Section 3.2, sliding variable s can reach the sliding surface $s = 0$ in fixed time. Once the estimate error e_{n-i}^i achieves stable in finite time, it follows from (8) and (9) that the tracking error dynamics are governed by

$$\begin{aligned} e^{[i]} &= e^{[i+1]}, \quad i = 0, \dots, n-1, \\ e^{[n]} &= - \int_0^\sigma \sum_{i=0}^{n-1} l_i \operatorname{sgn} e^{[i]} |e^{[i]}|^{\omega_i} d\sigma. \end{aligned} \tag{20}$$

Then from Lemma 2, system (20) is finite-time stable, and the tracking error e can converge to zero in finite time. The proof is completed. \square

Remark 5. Here we only consider the finite-time control of nonlinear systems with uncertainty. For controller design of nonlinear systems, there are many other problems should be considered, state and control constraints, unmeasure states, and so on. It is very important to consider state and control constraints at the level of control design, especially for the engineering systems, if they are not taken into account, the performance of the system will be degraded, even become unstable. Barrier Lyapunov function, model predictive control and optimal control are applied to solve the state and control constraints [3,3,4,13,30]. A variant nonsmooth maximum principle was proposed for optimal control problems with both pure state and mixed constraints in [4]. Moreover, in [3], a variant nonsmooth maximum principle for state constrained problems was developed, where the results were also sufficient conditions of optimality for the normal linear-convex problems.

4 Simulation

To evaluate the effectiveness of the designed control scheme, two examples are given below. One is the second-order system, and another is the application to the tracking control problem of HSV in cruise phase.

Example 1. The nonlinear uncertain system is considered as follows:

$$\begin{aligned} \dot{x}_1 &= x_2 + d_1(x, t), \\ \dot{x}_2 &= \cos x_2 + x_2 + \log(1 + x_1^2) + u + d_2(x, t), \\ y &= x_1 \end{aligned}$$

with the following mismatched and matched disturbances [16, 22]:

$$d_1(x, t) = \begin{cases} x_1 + \sin x_1, & 0 \leq t < 15, 25 \leq t \leq 35, \\ x_1 + \sin x_1 + 2, & 15 \leq t < 25, \\ x_1 + \sin x_1 + 0.5 \sin t, & t > 35, \end{cases}$$

$$d_2(x, t) = \begin{cases} x_1^3 + \sin x_2, & 0 \leq t < 15, 25 \leq t \leq 35, \\ x_1^3 + \sin x_2 + 1, & 15 \leq t < 25, \\ x_1^3 + \sin x_2 + 0.6 \cos t, & t > 35. \end{cases}$$

For the better demonstration of the designed MPR law-based control scheme, the compared simulations with other two methods that are single power reaching (SPR) law-based control scheme and double power reaching (DPR) law-based control scheme are carried out. The SPR law and DPR law are as follows:

$$\begin{aligned} \text{SPR: } \dot{s} &= -k_1 |s|^{\omega_1} \text{sgn } s - k_4 s; \\ \text{DPR: } \dot{s} &= -k_1 |s|^{\omega_1} \text{sgn } s - k_2 |s|^{\omega_2} \text{sgn } s - k_4 s. \end{aligned}$$

During the simulation, the controller parameters of three control methods are given in Table 1. The parameters of sliding mode surface are $\alpha_0 = 9/11, \alpha_1 = 27/53, \alpha_2 = 27/40, l_0 = 8, l_1 = 7$, and the parameters of the observer are $L_1 = 10, L_2 = 40, \eta_0^1 = 11, \eta_1^1 = 13, \eta_2^1 = \eta_0^2 = 12, \eta_1^2 = 23$.

Table 1. Controller parameters of three control strategies.

SPR	DPR	MPR
$k_1 = 6$	$k_1 = 6$	$k_1 = 6$
$\omega_1 = 1.8$	$\omega_1 = 1.8$	$\omega_1 = 1.8$
	$k_2 = 5$	$k_2 = 5$
	$\omega_2 = 0.06$	$\omega_2 = 0.06$
		$k_3 = 5$
$k_4 = 8$	$k_4 = 8$	$k_4 = 8$

Remark 6. The parameters of the MPR law (3) are chosen to satisfy $c_i > 0, i = 1, \dots, 4, \beta_1 > 1, 0 < \beta_2 < 1,$

$$\beta_3 = \begin{cases} \max\{\beta_1, |s|\}, & |s| \geq 1, \\ \min\{\beta_2, |s|\} & \text{else.} \end{cases}$$

Based on the reachability analysis of the sliding variable s , the larger the parameters c_4, β_1 and the smaller the parameter β_2 , the faster the reachability of the sliding variable s . Thus, the faster convergence of tracking error is obtained. Moreover, the parameters of the sliding surface (9) are chosen to yield $\omega_{i-1} = \omega_i \omega_{i+1} / (2\omega_{i+1} - \omega_i) (i = 2, \dots, n), \omega_{n+1} = 1, \omega_n = \omega_0 \in (1 - \varepsilon, 1), \varepsilon \in (0, 1), l_i > 0 (i = 0, 1, \dots, n - 1),$ and the polynomial $\lambda^{n-1} + l_{n-1}\lambda^{n-2} + \dots + l_1\lambda + l_0$ is Hurwitz. As shown in (20), the parameters of the designed sliding surface (9) directly affect the convergence rate of the tracking error. At last, the larger the parameters of the FTDO (11), the faster the convergence and the higher estimation accuracy. They indirectly affect the convergence of the tracking error as given in (19). Based on the simulation results, when designing above parameters, the trade-off should be made to achieve the best control performance.

Simulation results are shown in Figs. 1–3. For the better demonstration of the simulation results, the local time simulation results are also given.

As shown in Fig. 1, under the same controller parameters, the DPR law-based control strategy and MPR law-based control strategy assures the stable tracking of output in the presence of the matched and mismatched disturbances. The MPR law-based control strategy achieves the stable tracking of x_1 in about 1 second and the tracking error converges to zero in finite time. Whereas, the stable time of DPR law-based control strategy is in about 2.5 seconds. And the SPR law-based control strategy achieves the most poor tracking performance. As can be seen from Fig. 2 that the control input is smooth and no chattering occurs under three control schemes. Moreover, in the presence of uncertainty, the sliding variable under MPR law reaches the sliding surface $s = 0$ in finite time and

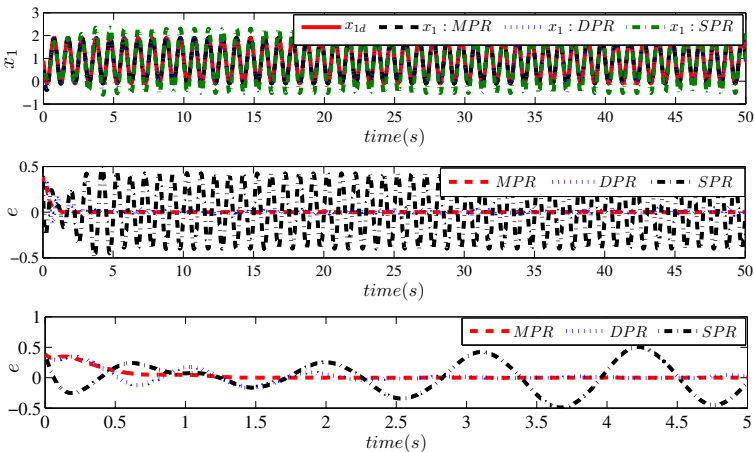


Figure 1. Time history of output tracking.

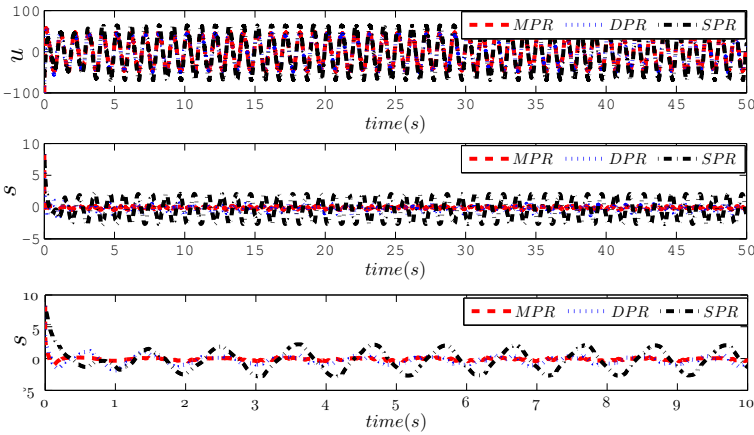


Figure 2. Time history of control input and the sliding state.

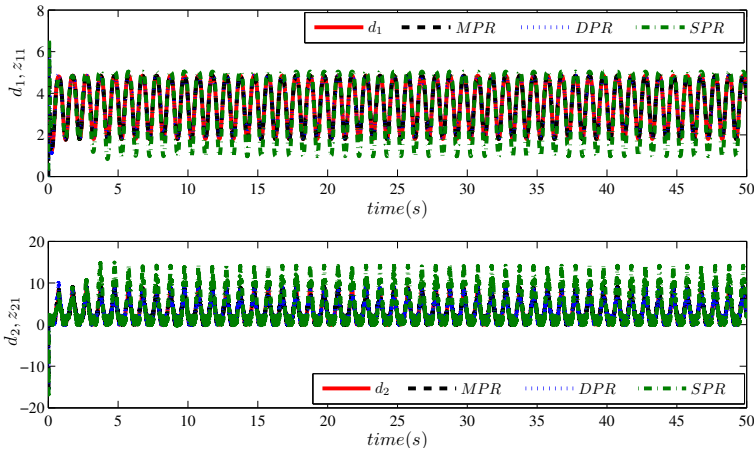


Figure 3. Time history of the disturbance estimate.

keeps stable in equilibrium point and no chattering occurs. And other two laws only reach the region around $s = 0$, the region of SPR law is larger than that of DPR law. It shows that the reaching performance of the MPR is better than those of other two reaching laws. It can be seen from Fig. 3 that the FTDO possess a good estimate performance under three control schemes.

From above analysis, the following conclusion can be obtained.

(a) The designed control scheme achieves the stable tracking of output under uncertainty in finite time, and it behaves good robustness via using FTDO. In addition, the chattering problem coherent in traditional SMC is effectively avoided.

(b) Compared with other two control schemes (DPR law-based control scheme and SPR law-based control scheme), the designed control scheme has the fastest convergence

rate and the highest tracking accuracy under the same design parameters and simulation conditions.

The simulation result verifies the theoretical results mentioned in previous section.

Example 2 [Application to HSV]. To further testify the effectiveness of the proposed control strategy, the altitude and velocity tracking control problem of HSV in cruise phase is shown as follows. The longitudinal dynamic equations of HSV are [34]

$$\begin{aligned} \dot{V} &= \frac{T \cos \alpha - D}{m} - g \sin \gamma, & \dot{h} &= V \sin \gamma, \\ \dot{\gamma} &= \frac{L + T \sin \alpha}{mV} - \frac{g \cos \gamma}{V}, & \dot{\alpha} &= q - \dot{\gamma}, \\ \dot{q} &= \frac{M_{yy}}{I_{yy}}, & \ddot{\eta}_i &= -2\xi_i \omega_i \dot{\eta}_i - \omega_i^2 \eta_i + N_i, \quad i = 1, 2, 3, \end{aligned} \quad (21)$$

where V, h, γ, α, q represents velocity, altitude, flight path angle (FPA), angle of attack (AOA) and pitch rate. Besides, L, D, T, M_{yy}, N_i ($i = 1, 2, 3$) are lift, drag, thrust, pitching moment and the generalized forces, which are complex functions of states and inputs. The approximations of the forces and moments and the coefficients are referred to [21].

The control goal is to design the controller to assure that V and h track the given reference signals V_{ref} and h_{ref} with aerodynamic uncertainty, where the flexible dynamics are not taken into account directly at the level of control design, but are considered as perturbations on the rigid body equations, and their effects are evaluated in the simulation. By the same token in [9, 31, 41], the controller for altitude and velocity is developed separately from the engineering backgrounds of HSV. Dynamic (21) can be transformed into the following form:

$$\dot{V} = f_V + g_V \phi + \Delta f_V, \quad (22)$$

$$\begin{aligned} \dot{h} &= V \sin \gamma, & \dot{\gamma} &= \alpha + \Delta f_\gamma, \\ \dot{\alpha} &= q + \Delta f_\alpha, & \dot{q} &= f_q + g_q \delta_e + \Delta f_q. \end{aligned} \quad (23)$$

In above equations, $\Delta f_V, \Delta f_\gamma, \Delta f_\alpha$ and Δf_q are unknown, and the detail for them can be referred to [31], which can be estimated by the FTDO.

On the basis of the preceding section, the control inputs for (22) and (23) are as follows:

$$\begin{aligned} u_v &= -g_v^{-1} \left[f_v + \Delta \hat{f}_v - V_{\text{ref}} + \sum_{i=1}^3 k_{vi} |s_v|^{\beta_{vi}} \text{sgn } s_v + k_{v4} s_v \right] \\ u_h &= -g_q^{-1} \left[f_q + \Delta \hat{f}_\gamma^{[3]} + \Delta \hat{f}_\alpha^{[2]} + \Delta \hat{f}_q^{[1]} - h_{\text{ref}}^{[4]} + k_{h4} s_h \right. \\ &\quad \left. + \sum_{i=0}^3 l_{hi} \text{sgn } e_h^{[i]} |e_h^{[i]}|^{\omega_{hi}} + \sum_{i=1}^3 k_{hi} |s_h|^{\beta_{hi}} \text{sgn } s_h \right], \end{aligned}$$

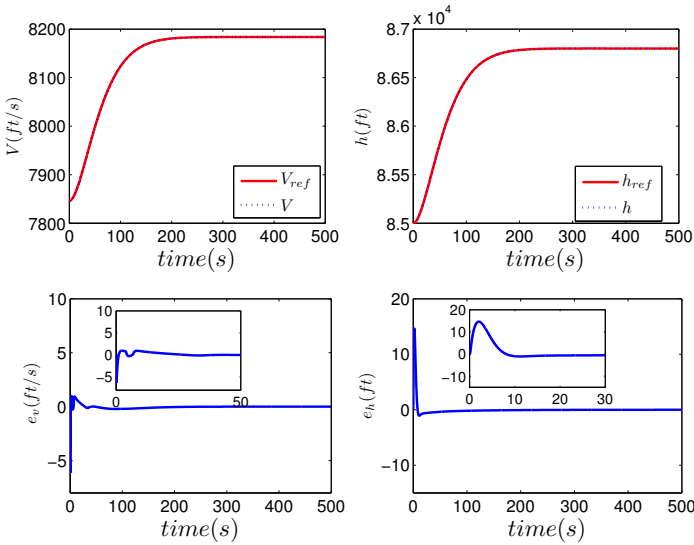


Figure 4. Time response of velocity and altitude tracking.

where $s_v = e_v = V - V_{ref}$ and $e_h = h - h_{ref}$ are the tracking errors of velocity and altitude, respectively. Besides, the sliding surface for altitude is $s_h = e_h^{[3]} + \int_0^\sigma (\sum_{i=0}^3 l_{hi} \operatorname{sgn} e_h^{[i]} |e_h^{[i]}|^{\omega_{hi}}) d\sigma$.

During the simulation, the flight mission is set as: the aircraft achieves a climbing maneuver under the constant dynamic pressure $\bar{q} = 2075.44$ psf, where altitude reference command h_{ref} is produced to make the aircraft climbs 1800 ft. At the same time, the velocity reference command V_{ref} is computed by $V_{ref} = (2\bar{q} \exp((h_{ref} - h_0)/h_s)/\rho_0)^{0.5}$. Moreover, the reference commands are brought out via a second-order pre-filter where a damping factor and a natural frequency are 0.95 and 0.03 rad/s, respectively. The fuel level of aircraft is 50 percent and the uncertainty of aerodynamic parameter are set to be +30 percent of the nominal case. Figures 4–6 describe the simulation results of the designed control scheme.

As presented in Figs. 4–6, the designed controller achieves the stable tracking of velocity and altitude with aerodynamic uncertainty. In detail, it can be observed from Fig. 4 that the corresponding maximum absolute values of velocity and altitude tracking errors are about less than 1 ft/s and 15 ft, respectively. And the designed control scheme makes velocity and altitude tracking their reference commands in about 30 seconds and 15 seconds, respectively. It is clear from Fig. 5 that the control inputs are smooth, and they are kept between 0.4 and 0.8, between -0.05 rad and 0.35 rad, respectively. And no chattering problem occurs. As shown in Fig. 6, the designed control scheme effectively handles the aerodynamics uncertainty of HSV, and the applied FTDO estimates the uncertainty caused by aerodynamic parameters in high estimation accuracy and fast estimation rate. (Here e_{f_v} , e_{f_γ} , e_{f_α} , e_{f_q} represent the estimate errors of Δf_v , Δf_γ , Δf_α , Δf_q , respectively.)

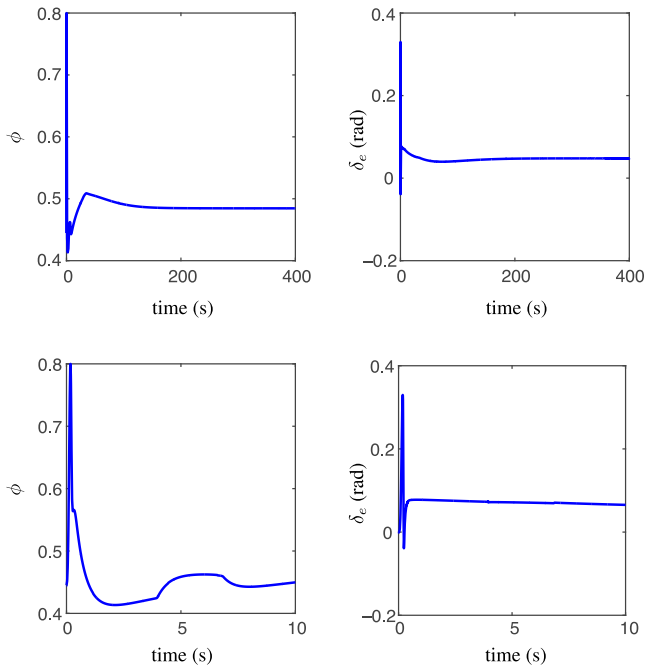


Figure 5. Time response of control inputs.

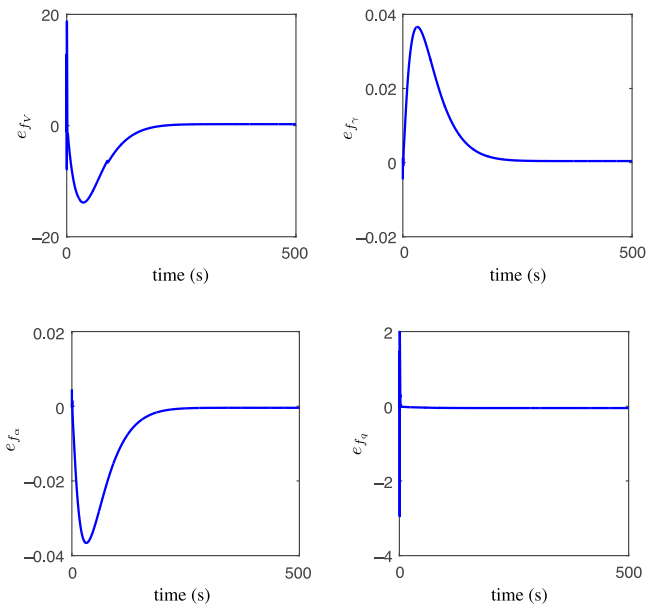


Figure 6. Time response of FTDO estimation error.

5 Conclusions

In this paper, combining MPR law and FTDO with SMC, the finite-time control scheme is proposed for uncertain nonlinear systems. The designed MPR law-based DOSMC scheme effectively avoids the chattering problem and achieves finite-time stability. Besides, the fixed-time feature of the MPR law is firstly analyzed. To sequel, the effectiveness of the developed control scheme is validated by a nonlinear system and the application of HSV tracking control problem. In future, we will focus on the finite-time control or optimal control of nonlinear systems with uncertainty, state and input constraints.

Acknowledgment. We would like to thank editor and all anonymous reviewers for their comments, which help to improve the quality of this paper.

References

1. S.P. Bhat, D.S. Bernstein, Finite-time stability of continuous autonomous systems, *SIAM J. Control Optim.*, **38**(3):751–766, 2000.
2. S.P. Bhat, D.S. Bernstein, Geometric homogeneity with applications to finite-time stability, *Math. Control Signals Syst.*, **17**(2):101–127, 2005.
3. M.H.A Biswas, M.d.R. de Pinho, A variant of nonsmooth maximum principle for state constrained problems, in *51st IEEE Conference on Decision and Control, December 10–13, 2012, Maui, HI, USA*, IEEE, 2012, pp. 7685–7690.
4. M.H.A. Biswas, M.d.R. de Pinho, A nonsmooth maximum principle for optimal control problems with state and mixed constraints, *ESAIM, Control Optim. Calc. Var.*, **21**(4):939–957, 2015.
5. J. Davila, L. Fridman, Observation and identification of mechanical systems via second order sliding modes, *Int. J. Control*, **76**(9–10):924–941, 2003.
6. F. Ding, J. Huang, Y.J. Wang, J.M. Zhang, Sliding mode control with an extended disturbance observer for a class of underactuated system in cascaded form, *Nonlinear Dyn.*, **90**(4):2571–2582, 2017.
7. A. Edwards, Y.B. Shtessel, Adaptive continuous higher order sliding mode control, *Automatica*, **65**(C):183–190, 2016.
8. Y. Feng, X.H. Yu, Z.H. Man, Non-singular terminal sliding mode control of rigid manipulators, *Automatica*, **38**(12):2159–2167, 2012.
9. L. Fiorentini, A. Serrani, M.A. Bolender, D.B. Doman, Nonlinear robust adaptive control of flexible air-breathing hypersonic vehicles, *J. Guid. Control Dyn.*, **78**(2):401–415, 2009.
10. L. Fridman, J.A. Moreno, B. Bandyopadhyay, S. Kamal, A. Chalanga, Continuous terminal sliding-mode controller, *Automatica*, **69**:308–314, 2016.
11. D. Ginoya, P.D. Shendge, S.B. Phadke, Sliding mode control for mismatched uncertain systems using an extended disturbance observer, *IEEE Trans. Ind. Electron.*, **61**(4):1983–1992, 2014.
12. D.A. Haghghi, S. Mobayen, Design of an adaptive super-twisting decoupled terminal sliding mode control scheme for a class of fourth-order systems, *ISA Trans.*, **75**:216–225, 2018.

13. W. He, Z. Yin, C. Sun, Adaptive neural network control of a marine vessel with constraints using the asymmetric barrier Lyapunov function, *IEEE Trans. Cybern.*, **47**(7):1641–1651, 2017.
14. S. Kamal, J.A. Moreno, A. Chalanga, B. Bandyopadhyay, L.M. Fridmand, Continuous terminal sliding-mode controller, *Automatica*, **69**:308–314, 2016.
15. A. Khanzadeh, M. Pourgholi, Fixed-time sliding mode controller design for synchronization of complex dynamical networks, *Nonlinear Dyn.*, **88**(4):2637–2649, 2017.
16. A. Levant, Higher-order sliding modes, differentiation and output-feedback control, *Int. J. Control*, **76**(9-10):924–941, 2003.
17. S. Mondal, C. Mahanta, Chattering free adaptive multivariable sliding mode controller for systems with matched and mismatched uncertainty, *ISA Trans.*, **52**:335–341, 2013.
18. A. Polyakov, Nonlinear feedback design for fixed-time stabilization of linear control systems, *IEEE Trans. Autom. Control*, **57**(8):2106–2110, 2012.
19. Y. Shtessel, C. Edwards, S. Spurgeon, J. Kochalummootil, Adaptive finite reaching time control and continuous second order sliding modes, in *Proceedings of the 49th IEEE Conference on Decision and Control*, IEEE Conference on Decision and Control, IEEE, Atlanta, GA, USA, 2010, pp. 5126–5131.
20. Y.B. Shtessel, I.A. Shkolnikov, A. Levant, Guidance and control of missile interceptor using second order sliding modes, *IEEE Trans. Aerosp. Electron. Syst.*, **45**(1):110–124, 2009.
21. D.O. Sighthorsson, A. Serrani, Development of linear parameter-varying models of hypersonic air-breathing vehicles, in *AIAA Guidance, Navigation and Control Conference, 10–13 August, 2009, Chicago, IL*, AIAA, Washington, DC, 2009, pp. 1–21.
22. H.B. Sun, S.H. Li, J. Yang, W.X. Zheng, Global output regulation for strict-feedback nonlinear systems with mismatched nonvanishing disturbance, *Int. J. Robust Nonlinear Control*, **10**(1002):3216–3231, 2014.
23. B.L. Tian, L.H. Liu, H.C. Lu, Z.Y. Zuo, Multivariable uniform finite-time out-put feedback reentry attitude control for RLV with mismatched disturbance, *IEEE Trans. Ind. Electron.*, **65**(3):2567–2577, 2018.
24. B.L. Tian, H.C. Lu, Z.Y. Zuo, Q. Zong, Multivariable finite-time output feedback trajectory tracking control of quadrotor helicopters, *Int J Robust Nonlinear Control*, **28**(1):281–295, 2018.
25. B.L. Tian, H.C. Lu, Z.Y. Zuo, Q. Zong, Multivariable uniform finite-time out-put feedback reentry attitude control for RLV with mismatched disturbance, *J. Franklin Inst.*, **335**(8):3470–3487, 2018.
26. B.L. Tian, L.P. Yin, H. Wang, Finite time reentry attitude control based on adaptive multivariable disturbance compensation, *IEEE Trans. Ind. Electron.*, **62**(9):5889–5898, 2015.
27. S.C. Tong, S. Sui, Y. Li, Fuzzy adaptive output feedback control of MIMO nonlinear systems with partial tracking errors constrained, *IEEE Trans. Fuzzy Syst.*, **23**(4):729–742, 2015.
28. E.V.I. Utkin, Variable structure systems with sliding modes, *IEEE Trans. Autom. Control*, **22**(2):212–222, 1977.
29. E.V.I. Utkin, Sliding mode control design principles and applications to electric drives, *IEEE Trans. Ind. Electron.*, **40**(1):23–36, 1993.

30. S.S. Vaddi, P. Sengupta, Controller design for hypersonic vehicles accommodating nonlinear state and control constraints, *IEEE Trans. Cybern.*, **47**(7):1641–1651, 2017.
31. F. Wang, Q. Zou, C.C. Hua, Q. Zong, Disturbance observer-based dynamic surface control design for a hypersonic vehicle with input constraints and uncertainty, *PIMechE Part I, J. Syst. Control Eng.*, **230**(6):522–536, 2016.
32. S. Wang, D. Yu, D. Yu, Compensation for unmatched uncertainty with adaptive RBF network, *Int. J. Eng. Sci. Technol.*, **3**(6):35–43, 2011.
33. C.C. Wen, C.C. Cheng, Designing of sliding surface for mismatched uncertain systems to achieve asymptotical stability, *J. Franklin Inst.*, **345**(8):926–941, 2008.
34. T. Williams, M.A. Bolender, D.B. Doman, O. Morataya, An aerothermal flexible mode analysis of a hypersonic vehicle, in *Proceedings of AIAA Atmospheric Flight Mechanics Conference and Exhibit, 21–24 August, 2006, Keystone, CO, AIAA, Washington, DC, 2006*, pp. 1–22.
35. J. Yang, S.H. Li, J.Y. Su, X.H. Yu, Continuous nonsingular terminal sliding mode control for systems with mismatched disturbances, *Automatica*, **49**:2287–2291, 2013.
36. J. Yang, S.H. Li, X.H. Yu, Sliding-mode control for systems with mismatched uncertainties via a disturbance observer, *IEEE Trans. Ind. Electron.*, **60**(1):160–169, 2013.
37. D.Y. Yao, R.Q. Lu, H.R. Ren, Sliding mode control for state-delayed Markov jump systems with partly unknown transition probabilities, *Nonlinear Dyn.*, **91**(1):475–486, 2018.
38. J.Y. Yao, W.X. Deng, Active disturbance rejection adaptive control of uncertain nonlinear systems: Theory and application, *Nonlinear Dyn.*, **89**(3):1611–1624, 2017.
39. S.H. Yu, X.H. Yu, B. Shirinzadeh, Z.H. Man, Continuous finite-time control for robotic manipulators with terminal sliding mode, *Automatica*, **41**(11):1957–1964, 2005.
40. Y. Zhang, G.F. Ma, Y.N. Guo, T.Y. Zeng, A multi power reaching law of sliding mode control design and analysis, *Acta Autom. Sin.*, **42**(3):466–472, 2016.
41. Q. Zong, F. Wang, B.L. Tian, Robust adaptive dynamic surface control design for a flexible air-breathing hypersonic vehicle with input constraints and uncertainty, *Nonlinear Dyn.*, **78**(1): 289–315, 2014.